JOURNAL OF NEUROTRAUMA 36:2233–2245 (July 15, 2019)

DOI: 10.1089/neu.2018.6036

Positive Allosteric Modulation of Cholinergic Receptors Improves Spatial Learning after Cortical Contusion Injury in Mice

Daniel P. Holschneider,[1–3] Yumei Guo,[1] Zhuo Wang,[1] Milagros Vidal,[1] and Oscar U. Scremin[3,†]

Abstract

We examined benzyl quinolone carboxylic acid (BQCA), a novel M1 muscarinic-positive allosteric modulator, for improving memory and motor dysfunction after cerebral cortical contusion injury (CCI). Adult mice received unilateral motorsensory cortical CCI or sham injury. Benzyl quinolone carboxylic acid (BQCA; 5, 10, and 20 mg/kg, intraperitoneally [i.p.] × 2/day × 3–4 weeks) or vehicle (Veh) were administered, and weekly evaluations were undertaken using a battery of motor tests, as well as the Morris water maze. Thereafter, cerebral metabolic activation was investigated in awake animals during walking with [^{14}C]-2-deoxygIucose autoradiography, comparing CCI mice previously treated with BQCA (20 mg/kg) or vehicle. Relative changes in local cerebral glucose uptake (rCGU) were evaluated in three-dimensional–reconstructed brains using statistical parametric mapping. CCI resulted in mild hyperactivity in the open field, and modest significant motor deficits, as well as significantly decreased spatial learning at 3 weeks. BQCA in CCI mice resulted in significantly improved spatial recall during the third week, with minimal effects on motor outcomes. CCI significantly decreased rCGU in the ipsilesional basal ganglia-thalamocortical circuit and in somatosensory regions, with relative increases noted contralaterally, as well as in the cerebellum. Significant decreases in rCGU were noted in subregions of the ipsilesional hippocampal formation, with significant increases noted contralesionally. BQCA compared to vehicle-treated mice showed modest, though significantly increased, rCGU in motor regions, as well as a partial reversal of lesion-related rCGU findings in subregions of the hippocampal formation. rCGU in ipsilesional posterior CA1 demonstrated a significant inverse correlation with latency to find the submerged platform. BQCA at 20 mg/kg had no significant effect on general motor activity, body weight, or acute motor, secretory, or respiratory symptoms. Results suggest that BQCA is a candidate compound to improve learning and memory function after brain trauma and may not suffer the associated central nervous system side effects typically associated with even modest doses of other cholinergic enhancers.

Keywords: acetylcholine; cerebral metabolism; cholinergic; cortical contusion injury; memory; mice; motor function; positive allosteric modulators; spatial navigation; traumatic brain injury

Introduction

It has long been known that central cholinergic mechanisms are essential to learning and memory.[1] Cholinergic pathways are disrupted both acutely and chronically in human traumatic brain injury (TBI) patients,[2] as well as in animal models of controlled cortical impact,[3] fluid percussion,[4–6] and blast injury.[7] Work from our lab has shown that acetylcholinesterase (AChE) inhibition reverses the cerebral ischemia present in TBI, possibly a key factor in reduction of the morphological extent of lesions. AChE inhibition enhances cerebral perfusion, an index of activation, on the contralateral symmetrical side, and significantly increases functional recruitment of the cerebellar thalamocortical pathway, subthalamic nucleus/zona incerta, red nucleus, and bilateral sensory cortex—all suggesting a beneficial effect on functional compensation.[8–10] Interest in exploration of the role of acetylcholine (ACh) in the pathophysiology and management of TBI has been growing in clinical therapeutic trials,[11–15] but questions remain about mechanisms of action and design of effective treatments. Inhibition of enzymatic degradation of ACh by inhibition of AChE appears as a

Departments of [1]Psychiatry and the Behavioral Sciences and [2]Neurology, Biomedical Engineering, University of Southern California, Los Angeles, California.
[3]Greater Los Angeles VA Healthcare System, Los Angeles, California.
[†]Deceased.

logical approach. However, translation to the clinical arena has been met with modest, though consistent, success.[13–15] Crucially, undesirable toxic effects of AChE inhibition have limited increased dosing during cholinomimetic therapy.[11,16–18] Peripheral and central distribution of this enzyme are so wide, and the functions of ACh so distributed, that side effects are common and pose a challenge to the efficient use of higher doses of the AChE inhibitors. Similarly, administration of muscarinic or nicotinic agonists may also lead to nonspecific activation of cholinergic transmission in numerous regions of the brain that contain these receptors.[19]

Recent work has launched the development of positive allosteric modulators (PAMs) of cholinergic receptors.[20–22] PAMs bind to allosteric sites where they have no effect alone, but increase the affinity and/or efficacy of endogenous ACh. Because PAMs do not directly activate the receptor, but instead potentiate activation by orthosteric ligands, they maintain the temporal and spatial signaling of cholinergic circuits. Benzylquinolone carboxylic acid (BQCA) is a highly selective M1 muscarinic PAM that shows no activity at muscarinic receptor subtypes M2–M5. BQCA has been reported to potentiate 47-fold the responsiveness of M1 agonists at a 10-mM concentration *in vitro*, with no activity at muscarinic receptor subtypes M2–M5.[23] This selectivity promises a substantially lower incidence of undesirable toxic effects during cholinomimetic therapy, and an improved means for counteracting neurocognitive and motor deficits.[19] Studies *in vivo* have established improvement of spatial memory in rodents at doses between 10 and 30 mg/kg intraperitoneally (i.p.).[23,24] In rats, BQCA reverses scopolamine-induced memory deficits,[23,25,26] deficits in reversal learning,[24] and time-induced disruption of object recognition.[27] PAMs improve cognitive performance also in the macaque.[26] However, to date, muscarinic PAMs have not been evaluated in an animal model of TBI. The current study examines the potential of BQCA on improving memory and motor dysfunction in a mouse model of unilateral cortical contusion injury (CCI).

Methods

Animals

C57/BL6 male mice were purchased from Jackson Laboratories (Sacramento, CA) at the age of 4 months. Animals were housed at the vivaria of the University of Southern California, a vivaria approved by the Association for Assessment and Accreditation of Laboratory Animal Care. All protocols were approved by the Institutional Animal Care and Use Committee. Mice were habituated to the vivaria environment for 1 week before initiation of the experiments, with experimental design as outlined in Figure 1. CCI animals were divided into four groups receiving daily administration of BQCA at one of three doses (20 mg/kg, CCI-20; 10 mg/kg, CCI-10; 5 mg/kg, CCI-5) or vehicle (CCI-Veh). Sham animals received daily administration of vehicle only (SHAM-Veh).

Cortex contusion injury

Mice were anesthetized with isoflurane (2.5% induction, 1.3% maintenance in 30% oxygen, and 70% nitrous oxide). The head was mounted in a stereotaxic frame (Stereotactic Alignment System; David Kopf Instruments, Tujunga, CA), the skin was incised and reflected, and a 3.6-mm craniotomy fashioned over the right sensorimotor cortex. Body temperature was maintained at 37.0 ± 0.5°C. CCI injury was induced using a Leica Impact One Stereotaxic Impactor device (impact velocity of 5.25 m/sec, 3.0-mm-diameter impounder tip, dwell time 0.1 sec, depth 2.0 mm; Leica Biosystems Inc., Buffalo Grove, IL). Stereotaxic coordinates for the center of impact were anterior-posterior −1.0 mm, +2.5 mm lateral to bregma. After trauma, the galea and skin was sutured to cover the

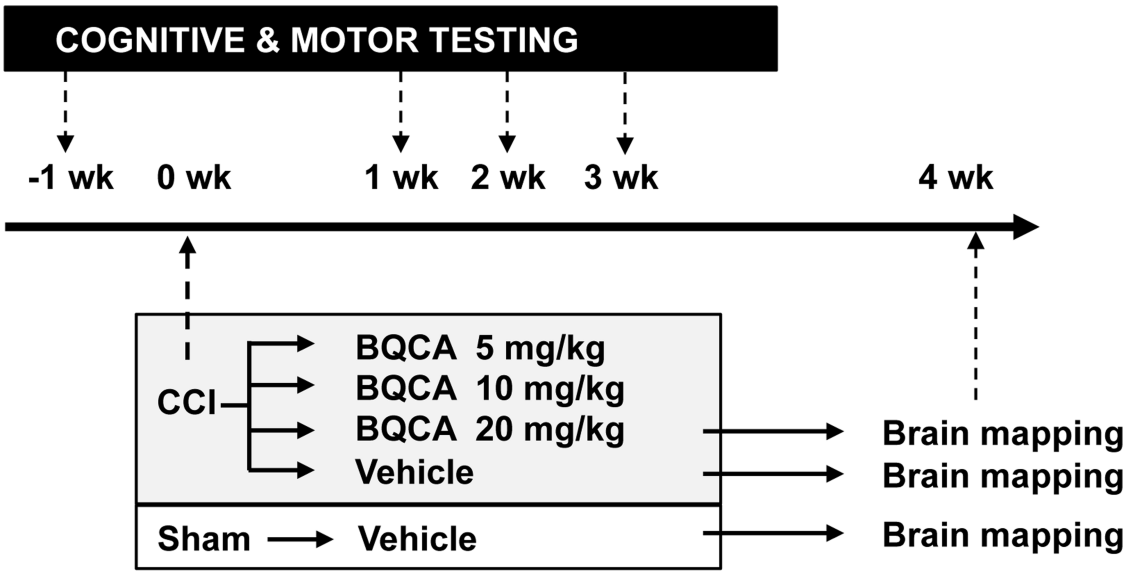

FIG. 1. Research design. Mice received right cortex contusion injury (CCI) over motorsensory cortex or sham injury (SHAM). Two days thereafter, they were administered benzyl quinolone carboxylic acid (BQCA; 5, 10, and 20 mg/kg, intraperitoneally), an M1 muscarinic-positive allosteric modulator, or vehicle. One week after CCI, mice were evaluated weekly for 3 weeks with a battery of motor tests, as well as with daily evaluation of spatial learning and memory using the Morris water maze. Thereafter, cerebral glucose uptake was investigated during walking in an exercise wheel with [^{14}C]-2-deoxygIucose autoradiography, comparing CCI mice treated with BQCA (20 mg/kg) or vehicle.

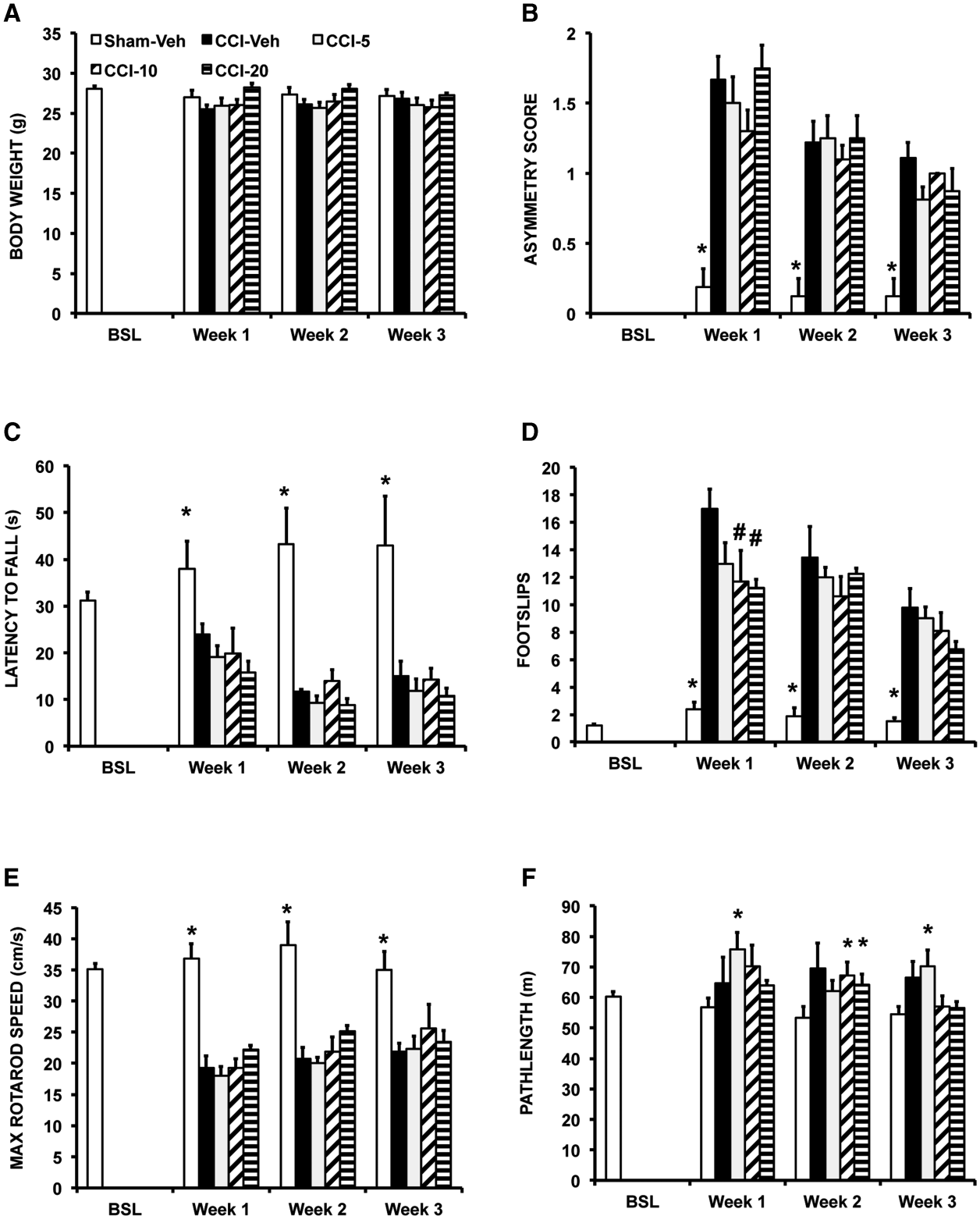

FIG. 2. Effects of CCI and BQCA on postural and motor outcomes. Mice were evaluated at baseline and weekly thereafter after CCI or SHAM-CCI. Mice received either vehicle (SHAM-Veh; CCI-Veh) or BQCA at one of three doses (CCI-5, 5 mg/kg; CCI-10, 10 mg/kg; CCI-20, 20 mg/kg; given intraperitoneally × 2/day) across a 3-week follow-up period. Shown are group means (± SEM) for (**A**) body weight. (**B**) Postural reflex asymmetry score, (**C**) Grip strength as indicated by latency to fall from an inverted grid, (**D**) Foot slips recorded on a grid over 5 min. (**E**) Maximum speed achieved on the accelerating rotarod. (**F**) Path length in the open field over 20 min. *Indicates at each specified time point, a significant difference of SHAM-Veh compared to CCI-5, CCI-10, or CCI-20 ($p < 0.05$). #Indicates significant difference of CCI mice receiving BQCA relative to their vehicle counterparts. BQCA, benzyl quinolone carboxylic acid; BSL, baseline; CCI, cortex contusion injury; SEM, standard error of the mean; Veh, vehicle.

craniotomy. In sham CCI, there was a skin incision, but no craniotomy. Mice were housed individually for 1 h in a warming/induction chamber at 37.0 ± 0.5°C (VWR, Radnor, PA) in a temperature-controlled cage to prevent hypothermia until they regained the righting reflex and spontaneous movements. Flunixin (2.5 mg/kg, subcutaneously × 2/day × 3 days) was administered for analgesia.

Administration of benzylquinolone carboxylic acid

Two days after CCI, mice were administered BQCA (98.6% purity by chromatography; Cayman Chemicals, Ann Arbor, MI), an M1 muscarinic positive allosteric modulator or vehicle. After CCI, animals received i.p. dosing at 5, 10, and 20 mg/kg (CCI-5, CCI-10, and CCI-20) in 0.1 mL of 10% Tween, with dosing twice per day over 31 days, and the first daily dose given 30 min before behavioral testing. Doses were prepared freshly before each injection. After i.p. injection, BQCA reaches a peak in brain 30 min to 1 h and remains stable for ~4 h, decaying thereafter with an elimination half-life of 2 h.[24] Doses of BQCA are based on previous reports in non-TBI models.[23–25,27]

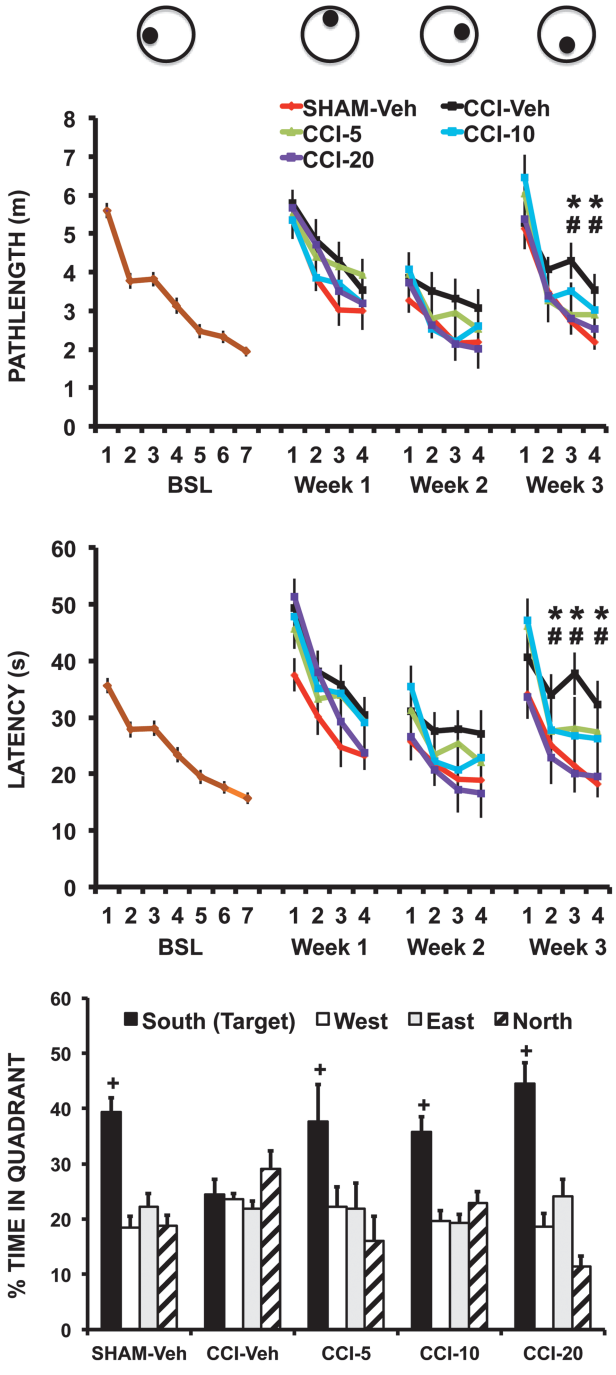

FIG. 3. Effects of CCI and BQCA on spatial learning and memory in the Morris water maze. Mice were trained at baseline (BSL) for 7 days (6 trials/day) and then weekly (4 days/week) for 3 weeks after CCI or sham CCI. The target platform was moved to a new position at the start of each week (see top schematic). Mice received either vehicle (SHAM-Veh, CCI-Veh) or BQCA at one of three doses (CCI-5, 5 mg/kg; CCI-10, 10 mg/kg; CCI-20, 20 mg/kg; given intraperitoneally × 2/day). Top and middle graphs show, respectively, the group mean path length and latency (± SEM) traveled to find the submerged platform during each phase of the study. Baseline (BSL; brown color) includes data from all animals. *CCI- Veh versus SHAM-Veh, $p < 0.05$; #CCI-20 versus CCI-Veh, $p < 0.05$. The bottom graph shows the percent time (± SEM) spent during the probe trial at the end of week 3 searching in the quadrant (South), which previously had contained the platform. +Significant difference ($p < 0.05$) between the CCI-Veh group compared to SHAM-Veh, CCI-5, CCI-10, and CCI-20 groups. BQCA, benzyl quinolone carboxylic acid; CCI, cortex contusion injury; SEM, standard error of the mean; Veh, vehicle.

Cholinergic side effects

Motor, secretory, respiratory, and general symptoms were graded in a separate group of nonlesioned mice ($n = 4$), before and at half hour intervals over 90 min after administration of BQCA (20 mg/kg, i.p.) as per the scale of Jovic.[28] Sedative effects were also evaluated by continuous monitoring of locomotor activity in the open field as described below. Locomotor activity was assessed by video tracking over a half hour, 30 min after acute dosing with BQCA (20 mg/kg, i.p.) or vehicle.

Motor assessment

Before experimentation, mice were familiarized with the rotarod (5 min/day × 5 days) and gait analysis (2 exposures/day × 2 days) paradigms (Fig. 1). All mice were tested before CCI and then once per week thereafter for 3 weeks. Before testing, mice were placed into the testing room for 1 h (ambient sound 57 dB). Motor testing occurred in the following sequence: Postural reflex → Open field → Footslip → Grip Strength → Gait analysis → Rotarod. Comparison was made between SHAM-Veh ($n = 8$), CCI-Veh ($n = 9$), CCI-5 ($n = 8$), CCI-10 ($n = 10$), and CCI-20 (n = 8) groups.

Postural reflex.[29] This was assessed in a blinded fashion. Mice were lifted by their tails and recorded using a 3-point scale: 0 = hindlimb abduction, forelimb symmetric splayed apart, arched back (normal response); 1 = failure to extend the contralesional forepaw fully, with or without wrist flexion; and 2 = full adduction of forepaw, with shoulder rotation toward contralateral thorax.

Open field behavior. Locomotor activity was measured in a circular arena (diameter, 38.0 cm). Pathlength was recorded with a video tracking system (Ethovision XT; Noldus, Leesburg, VA) under attenuated yellow lighting using a ceiling-mounted camera. Trajectories during 20-min trials were recorded, as an indication of their locomotor behavior.

Footslip. Mice were individually placed in the test chamber, which consisted of a Plexiglas/stainless steel box (30 × 30 × 30 cm)

with a floor of stainless steel rods of 2-mm diameter and 1-cm separation. The chamber was illuminated with indirect ambient fluorescent light from a ceiling panel. A mouse was filmed for 5 min from below, while it walked on the grid. Footslips were counted offline from the video recording in a blinded fashion as a measure of fine motor coordination.

Gait analysis. Mice were trained to traverse a white, Plexiglas walkway (4 cm width, 15 cm height, and 46 cm height) to reach a black enclosed target box ($25 \times 25 \times 15$ cm). Feet were painted with different color nontoxic paint. Thereafter, the mouse was released to traverse the runway whose floor was covered with white paper (3 trials/day, 5-min intertrial interval) and which was illuminated with indirect ambient fluorescent light from a ceiling panel. Stride length, hind-paw stance width, and overlap of hind paws were assessed by ruler, excluding footprints at the beginning and end of the trials where mice initiated and finished their run, respectively. The average of three runs was taken as the animal's values for stride length, stance width (front-base width, hind-base width), and gait pattern (overlap between forepaw and hindpaw placement) using the methods of Carter and colleagues.[30]

Grip strength. Latency was measured to fall off of an inverted cage top into bedding below. The average of 3 trials was assessed (10-min intertrial interval).

Rotarod treadmill test. Strength and coordination were evaluated on a rotarod treadmill (Columbus Instruments, Columbus, OH). Mice were placed on a scored, cylindrical spindle of 7.3 cm diameter with lateral motion impeded by opaque plastic panels. Latency to fall was tested in an acceleration paradigm ($5 \rightarrow 35$ rpm over 300 sec in 1-rpm intervals, 3 trials/mouse, 5-min intertrial intervals), with the average of three runs representing the animal's performance.[31,32]

Spatial learning and memory

This was evaluated with a water maze paradigm,[33,34] comparing SHAM-Veh ($n=12$), CCI-Veh ($n=14$), CCI-5 ($n=8$), CCI-10 ($n=10$), and CCI-20 ($n=9$) groups. Mice swam in a circular pool surrounded by a white curtain to find a circular platform, submerged 1 cm beneath the water (20°C), opacified by the addition of white non-toxic paint. Visual cues mounted on the inside of the arena were in a constant position. Data were acquired under indirect ambient fluorescent lighting using a ceiling-mounted camera and video tracking system (Ethovision XT; Noldus). Mice were introduced into the maze alternating between starting positions orthogonal to the platform. A trial was stopped when the mouse reached the platform or if 60 sec elapsed, after which the mouse was placed on the platform. After remaining on the platform for 15 sec, the mouse was removed from the maze, gently towel-dried, and returned to its cage. At baseline preceding CCI, mice received 6 trials per day (intertrial interval 20 min) for 7 consecutive days, and then weekly (6 trials/day $\times$ 4 days/week) for 3 weeks after CCI or sham CCI. The target platform was moved to a new quadrant in the maze at the start of each week (reversal phase). In the final trial of the final week, recall was evaluated with a probe trial. Here, the escape platform was removed and the duration over 60 sec spent searching in the quadrant of the maze that previously held the platform was examined.

Behavioral data analysis

For grip strength, rotarod, foot slip, and gait analyses, we applied two-way, repeated-measures analyses of variance (ANOVAs; mixed-model ANOVA, SPSS, version 14.0) at weekly post-operative time points, using GROUP as the between-subjects variable and WEEKS as the within-subjects repeated measure. *t*-tests (two-tailed, $p<0.05$) were used for post-hoc comparisons. Postural asymmetry scores were compared between groups by the Kruskal-Wallis test at each time point.

For the water maze, latency and pathlength to reach the target were averaged across the 6 trials/day and expressed as a daily mean. Baseline data included all animals in the study. Two-way repeated-measures ANOVA was separately used to analyze the acquisition phase (baseline, days 1–7), as well as each of the weekly reversal phases (weeks 1–3, days 1–4). GROUP was defined as the between-subject variable and DAYS as the repeated measure. In addition, we examined in CCI animals the effects of different BQCA doses

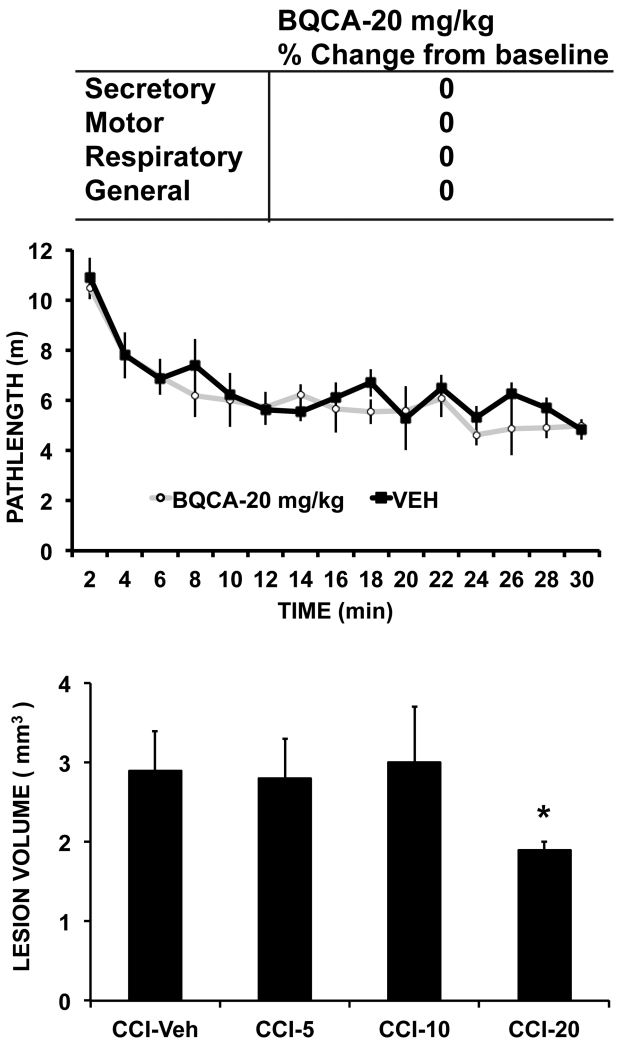

FIG. 4. Effect of BQCA on locomotor activity, cholinergic symptoms, and lesion volume. Locomotor activity counts were collected in non-lesioned animals in the open field for 30 min, 30 min after a single injection of BQCA ($n=4$, 20 mg/kg, intraperitoneally [i.p.]) or vehicle ($n=4$). Symptoms of acute cholinergic toxicity were evaluated over 90 min in response to BQCA ($n=4$, 20 mg/kg i.p.) using the scale of Jovic.[28] These included evaluation of secretory symptoms (lacrimation, eye protrusion, and salivation), motor symptoms (tremor, fibrillation, and fasciculation), respiratory changes, as well as general changes (body posture, reactivity). Lesion volume (average $\pm$ SE) was computed from digitized autoradiographs of serial coronal brain cryosections ($n=8$–10). *$p<0.05$ CCI-Veh versus CCI-20. BQCA, benzyl quinolone carboxylic acid; CCI, cortex contusion injury; SE, standard error; Veh, vehicle.

(vehicle, 5 mg/kg, 10 mg/kg, and 20 mg/kg). Repeated-measures one-way ANOVA was separately used to analyze each of the reversal phases (weeks 1–3, days 1–4), using DOSE as the between-subjects factor and DAYS as the within-subjects repeated measure. For the probe trial that followed the final reversal phase, the time spent in each of the maze's quadrants was assessed. Percent of time spent swimming by each animal in each quadrant was analyzed using a two-way ANOVA with GROUP as between-subjects variables and QUADRANT as the within-subjects repeated measure. *t*-tests (two-tailed, $p < 0.05$) were used for post-hoc comparisons.

Measurement of cerebral glucose uptake during a wheel walking motor challenge

Five days after the final evaluation in the water maze, CCI-Veh ($n = 9$), CCI-20 ($n = 8$), and SHAM-Veh ($n = 10$) mice were familiarized to slow walking in a closed motorized wheel for 5 min/day twice per day over 2 days (wheel diameter, 15.2 cm; interspoke distance, 6.6 mm; Lafayette Instruments, Lafayette, IN). Mice were fasted overnight on the day of the study, with the final dose of BQCA administered to the CCI-20 group 18 h before brain mapping. One hour after being brought to the experimental suite, mice were administered [^{14}C]-2-deoxy-D-glucose (catalog no. MC355, radiochemical purity >97%, specific activity 45–60 mCi/mmol, 0.3 μCi/g in 0.5 mL of normal saline, i.p.; Moravek Inc., Brea, CA). Animals were placed into the motorized wheel and walked at a speed of 2 m/min over 45 min. Thereafter, mice were anesthetized with isoflurane (4%) and decapitated.

Brains were flash frozen and serially sectioned (75 coronal 20-μm slices, 140-μm interslice distance). Autoradiographic images of brain slices along with 12 [^{14}C] standards (GE Healthcare Life Sciences, Pittsburgh, PA) were digitized. Relative regional cerebral glucose uptake (rCGU) was measured according to the method of Sokoloff and colleagues,[35] with modification.[36–38]

Lesion volume

After completion of the assessment rCGU and euthanasia, lesion volume was determined from digitized autoradiographs of serial coronal brain cryosections in a manner blinded to drug dosing. Contours of the area of tissue loss and of the ipsi- and contralateral hemispheres were drawn, and their respective areas were computed on slices with Image-Pro Plus (Media Cybernetics, Rockville, MD). Total volume of the lesion for each animal was computed by multiplying the average areas (μm^2) of every two consecutive slices by the interslice distance (140 μm).

Analysis of regional brain activation

Each three-dimensional (3D) brain was reconstructed from 75 digitized autoradiograms (voxel size: $40 \times 140 \times 40\ \mu m^3$) using TurboReg[39] and a non-warping geometric model that includes rotations and translations and nearest-neighbor interpolation. A brain template was created using our previously published methods,[40] in which the background and ventricular spaces were thresholded based on their optical density. We utilized cost-function masking for spatial normalization of lesioned brain.[41,42] Binary masks were created of the lesioned areas in each CCI animal by manually depicting the precise boundaries of any gross lesions directly on the autoradiographic images using MRIcron software. Signal under the masked area in each animal was removed from the calculation of the transformations needed to normalize the image in order to avoid distortion. Spatial normalization consisted of a 12-parameter affine transformation followed by a non-linear spatial normalization using 3D discrete cosine transforms. Normalized brains were smoothed with a Gaussian kernel (full width at half maximum = 3 × voxel dimension). Absolute amount of radiotracer of each brain was scaled to a single mean.

Unbiased, voxel-by-voxel statistical analyses were performed using statistical parametric mapping (SPM, version 5)[43] to identify significant group differences in relative changes in local glucose uptake (rCGU) during wheel walking for the CCI-Veh versus SHAM-Veh and the CCI-20 versus CCI-Veh comparisons. Significance was set at $p < 0.05$ at the voxel level and an extent threshold of greater than 100 significant, contiguous voxels to control type 1 and 2 errors. Regions were identified by a mouse brain atlas.[44] Directionality of rCGU changes was analyzed with Student's *t*-tests (2-tailed, $p < 0.05$, >100 voxels cluster size). In

FIG. 5. Effects of CCI and BQCA on regional brain glucose uptake (rCGU) during motor challenge. Significant group differences in functional brain activation during wheel walking for the CCI-Veh versus SHAM-Veh and the CCI-20 versus CCI-Veh comparisons. Representative coronal sections (anterior- posterior [AP] coordinates relative to the bregma in millimeters) depicting the ipsilesional (right) and contralesional (left) hemispheres. The color-coded statistical parametric maps superimposed on coronal images of the rCGU template brain show significant group differences, with red and blue colors showing positive and negative changes, respectively ($p < 0.05$ at the voxel level for clusters of >100 contiguous voxels, $n = 8$–10 per group). BQCA, benzyl quinolone carboxylic acid; CCI, cortex contusion injury; Veh, vehicle.
Abbreviations:

Acb, accumbens nucleus
AH, anterior hypothalamus
APT, anterior pretectal area
Au, auditory cortex
BLA, basolateral amygdaloid n.
CA1/CA2, hippocampus CA1/CA2
Ce, central amygdaloid n.
Cg, cingulate cortex
CM, central medial thalamic n.
CPu, striatum
DG, dentate gyrus
La, lateral amygdaloid n.
LD, lateral dorsal thalamic n.
GPE, external globus pallidus
IC, inferior colliculus
Ins, insula
Int, intermediate deep cerebellar n.
La, lateral amygdala
Lat, lateral deep cerebellar n.
ll, lateral lemniscus
M1, primary motor cortex
Med, medial deep cerebellar n.
mfb, median forebrain bundle
MG, medial geniculate
PAG, periaqueductal gray
PB, parabrachial n.
Pir, piriform cortex
PMCo, cortical amygdaloid n.
Pn, pons
Po, posterior n. thalamic n.
RN, red nucleus
RS, retrosplenial cortex
RT, reticular thalamic n.
S1/S2, primary/secondary somatosensory cortex
SC, superior colliculus
Sim, intermediate lobule of the cerebellum
SN, substantia nigra
V2, secondary visual cortex
Ve, vestibular n.
VL, ventrolateral thalamic n.
VM, ventromedial thalamic n.
VPL/VPM ventroposterior lateral/ventroposterior medial thalamic n.
ZI, zona incerta

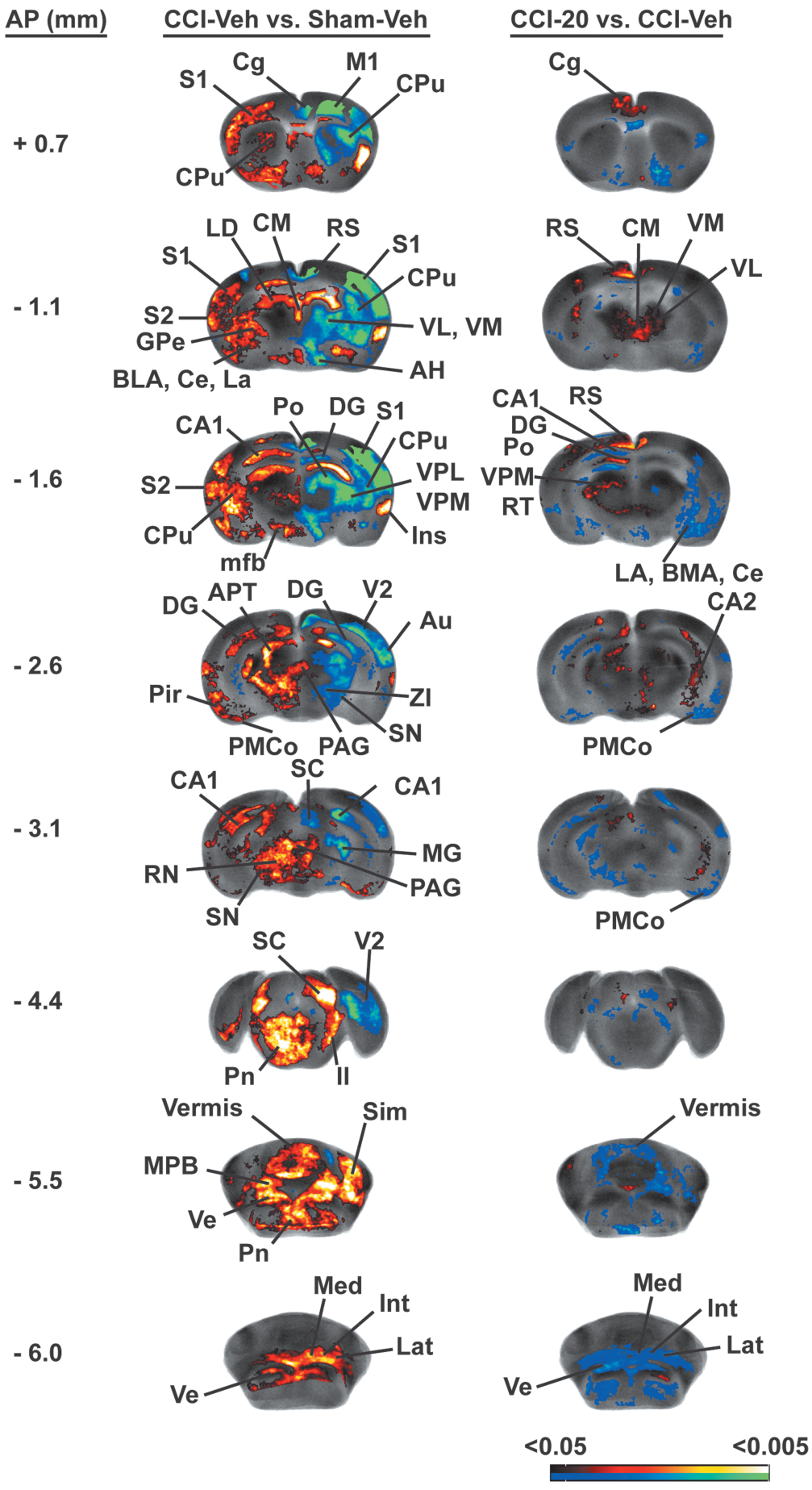
AP (mm)
CCI-Veh vs. Sham-Veh
CCI-20 vs. CCI-Veh
+ 0.7
Cg
M1
S1
CPu
CPu
Cg
- 1.1
LD
CM
RS
S1
S1
CPu
S2
VL, VM
GPe
AH
BLA, Ce, La
RS
CM
VM
VL
- 1.6
CA1
Po
DG
S1
CPu
S2
VPL
VPM
CPu
Ins
mfb
CA1
RS
DG
Po
VPM
RT
LA, BMA, Ce
- 2.6
DG
APT
DG
V2
Au
Pir
ZI
PMCo
PAG
SN
CA2
PMCo
- 3.1
CA1
SC
CA1
MG
RN
PAG
SN
PMCo
- 4.4
SC
V2
Pn
II
- 5.5
Vermis
Sim
MPB
Ve
Pn
Vermis
- 6.0
Med
Int
Lat
Ve
Med
Int
Lat
Ve
<0.05
<0.005

TABLE 1. REGIONS SHOWING STATISTICALLY SIGNIFICANT DIFFERENCES OF FUNCTIONAL BRAIN ACTIVATION DURING MOTOR CHALLENGE

Cortex	*CCI-Veh versus SHAM-Veh (Contra/Ipsi)*	*CCI-20 versus CCI-Veh (Contra/Ipsi)*
Motor system		
Motor cortex, primary (M1)	↑ / ↓	
Motor cortex, secondary (M2)	/ ↓.	↑ / ↑
Caudate-putamen (CPu)	↑ / ↓	post: ↑ /
Cerebellum		
Interposed n.	↑ / ↑	↓ / ↓
Lateral n.	/ ↑.	↓ / ↓
Medial n.	↑ / ↑	↓ / ↓
Lateral lobe	↑ / ↑	/ ↓.
Vermis	↑	↓
Globus pallidus, external (GPe)	↑ / ↓	
Red nucleus (RN)	↑ / .	↓ /
Substantia nigra (SN)	↑ / .	↓ /
Subthalamic nucleus (STN)	/ ↓.	
Thalamus		
Central medial (CM)	↑	
Mediodorsal (MD), ventral anterior (VA)	/ ↓.	↑ /
Ventrolateral (VL), ventromedial (VM)	/ ↓	↑ / ↑
Zona incerta (ZI)	↑ / ↓	↓ /
Sensory system		
Auditory cortex (Au)	↑ / ↓	/ ↓
Piriform cortex (Pir)	↑ /	/ ↓
Somatosensory cortex, primary (jaw S1J, upper lip S1ULp, forelimb S1FL, dysgranular, S1DZ, barrel field S1BF)	↑ / ↓	↑ S1BF only /
Somatosensory cortex, secondary (S2)	↑ / ↓	/ ↓
Visual cortex, primary (V1)	/ ↓.	↑ /
Visual cortex, secondary (V2)	↑ / ↓	
Anterior pretectal area (APT)	/ ↓..	↑ /
Colliculus, inferior (IC)	↓ / ↓	/ ↑
Colliculus, superior (SC)	↑ / ↑	↑ /
Geniculate, dorsolateral (DLG)	↑ / ↓	
Thalamus		
Medial geniculate (MG)	/ ↓.	
Posterior (Po)	↑ / ↓	
Ventroposterior lateral (VPL)	↑ / ↓	↑ /
Ventroposterior medial (VPM)	↑ / ↓	↑ /
Vestibular nucleus (Ve)	↑ / ↑	↓ / ↓
Limbic-associated		
Cingulate cortex (Cg)	/ ↓	↑ / ↑
Dorsal peduncular cortex (DP)	↑ / ↑	
Entorhinal cortex	↑ /	↓ / ↓
Infralimbic cortex (IL)	↑ / ↑	/ ↓.
Insula cortex (Ins)	/ ↑	
Orbital cortex, lateral/ventral (LO/VO)	↑ / ↓	↑ / ↑
Prelimbic cortex (PrL)	/ ↓	↑ / ↑
Retrosplenial cortex	↓ / ↓	↑ /
Accumbens n. (Acb)	↑ / ↑	/ ↓.
Amygdala		
Basal	↑ / ↑	↓ / ↓
Central	↑ / ↓	/ ↓
Cortical	↑ /	/ ↓
Lateral	↑ / ↓	/ ↓
Medial	↑ /	↓ / ↓
Bed n. of the stria terminalis	/ ↓.	
Hippocampal formation		
CA1 anterior (ant), posterior (post)	ant: ↑ /, post: ↑ / ↓	ant: ↓ /, post: ↓ / ↑
CA2, CA3		post: / ↑
Dentate gyrus (DG), anterior (ant)	ant:↓ / ↓, post: ↑ /	ant: ↑ /
Subiculum, transition area (STr), post (Post), Pre (PrS)	↑ / ↓	

(*continued*)

TABLE 1. (CONTINUED)

Cortex	*CCI-Veh versus SHAM-Veh (Contra/Ipsi)*	*CCI-20 versus CCI-Veh (Contra/Ipsi)*
Hypothalamus		
Anterior (AH), lateral (LH)	↑ /	
Posterior (PH)	↑ / ↓	/ ↑.
Preoptic area, lateral (LPO), medial (MPA)	↑ /	
Ventromedial	↑ / ↓	↓ / ↓
Septal nucleus, lateral (LS)	↑ /	
Other		
Parabrachial n. (PB)	↑ / ↑	
Pons (Pn)	↑ / ↑	
Reticular formation (RtF)	↑ / ↑	
Thalamus		
Anterior dorsal, medial, ventral (AD, AM, AV)	/ ↓.	↑ / ↑
Lateral dorsal (LD)	/ ↓..	
Lateral posterior (LP)	↑ / ↓	
Paraventricular (PV)	↑	
Reticular (Rt)	↑ / ↓	↑ /

Comparison is between rats with right cortical contusion and sham-lesioned animals, receiving vehicle (CCI-Veh, $n=10$ vs. SHAM-Veh, $n=9$), as well as between CCI mice receiving BQCA (20 mg/kg, intraperitoneally i.p., $n=8$) and CCI mice receiving vehicle (CCI-Veh). Significant increases or decreases in glucose uptake are noted with '↑' and '↓', respectively, for the contra- and ipsilesional hemispheres. Significance is shown at the voxel level for $p<0.05$ for clusters >100 contiguous voxels. Abbreviations are taken from the Franklin and Paxinos mouse brain atlas.[55]

ant, anterior; post, posterior; CCI, cortical contusion injury; Veh, vehicle; BQCA, benzylquinolone carboxylic acid.

addition, using SPM, we performed a correlation between latency to find the platform on day 4 of the third week and rCGU across the brain ($p<0.05$ for >100 contiguous voxels) for the combined Sham-Veh, CCI-Veh, and CCI-20 groups. In addition, correlations of latency with rCGU from an ipsilesional and contralesional posterior CA1 region of interest are depicted graphically.

Results

Effect of lesion on body weight, postural reflexes, and behavior

Right unilateral CCI was not associated with a significant change in body weight (Fig. 2A). CCI resulted in a significant, asymmetric postural reflex on tail suspension at weeks 1–3 ($p<0.0005$; Fig. 2B). Lesioning resulted in a significant decrease in grip strength (GROUP, $F_{4,38}=9.5$; $p<0.04$; Fig. 2C), increase in footslips (GROUP, $F_{4,38}=29.0$; $p<0.0005$; Fig. 2D), and decrease in rotarod performance (GROUP, $F_{4,38}=10.2$; $p<0.0005$; Fig. 2E). Post-hoc testing revealed differences for the CCI-Veh versus SHAM-Veh comparison at weeks 1–3 (Fig. 2; $p<0.05$ to $p<0.0005$). CCI resulted in a nonsignificant decrease in stride length, stance width, or gait pattern (data not shown). CCI resulted in a nonsignificant trend toward hyperactivity in the open field (Fig. 2F).

During the acquisition phase in the water maze, escape latency and pathlength decreased significantly with repeated daily trials (DAYS: latency, $F_{6,312}=47.5$, $p<0.0005$; pathlength, $F_{6,312}=62.7$, $p<0.0005$). After CCI or sham-CCI, latency during week 3 differed significantly across GROUPS ($F_{4,48}=2.9$; $p<0.03$; Fig. 3), as well as across DAYS ($F_{3,144}=53.8$; $p<0.0005$; Fig. 3), with a significant GROUP×DAYS interaction ($F_{12,144}=2.5$; $p<0.006$; Fig. 3). Similarly, pathlength during week 3 after CCI or sham-CCI differed by GROUP ($F_{4,48}=3.0$; $p<0.03$), as well as across DAYS ($F_{3,144}=60.5$; $p<0.0005$), with a GROUP×DAYS interaction ($F_{12,144}=2.2$; $p<0.02$). Although there was a trend toward an effect of GROUP and GROUP×DAYS at weeks 1 and 2, it did not reach significance. Post-hoc testing revealed that CCI-Veh compared to SHAM-Veh showed significant increases during the third week in latency (week 3: days 2–4, $p<0.05$) and pathlength (week 3: days 3–4, $p<0.05$). There were no significant group differences in swim velocity at any time. During the probe trial (Fig. 3), the percentage of time spent swimming in the target quadrant that previously contained the platform was significantly increased (QUADRANT, $F_{3,129}=27.5$; $p<0.0005$), suggesting animals were searching for a previously learned platform position. Significant learning differed by group (QUADRANT× GROUP, $F_{12,129}=3.6$; $p<0.0005$), with post-hoc testing showing significantly decreased percent time in the target quadrant of the CCI-Veh group compared to each of the other groups.

Effect of benzylquinolone carboxylic acid on behavior

Lesion volume showed a significant ($p<0.05$) decrease in the CCI group receiving the highest dose of BQCA compared to the CCI group receiving vehicle (CCI-Veh $2.9\pm0.5\,mm^3$, CCI-5 $2.8\pm0.5\,mm^3$, CCI-10 $3.0\pm0.7\,mm^3$, and CCI-20 $1.9\pm0.1\,mm^3$). In CCI mice, acute administration of BQCA at 20 mg/kg had no significant effect on general motor activity in the open field (nonsignificant trend, $p<0.09$; Fig. 4) or on acute motor, secretory, or respiratory symptoms when assessed using the cholinergic toxicity scale of Jovic.[28] Chronic BQCA administration did not significantly change body weight (Fig. 2A) in CCI mice. Effects of chronic BQCA administration on motor outcomes (postural asymmetry, grip strength, footslip, and rotarod) were absent, with a nonsignificant trend to diminish CCI-related hyperactivity in the open field and a transitory effect on decreasing footslips during week 1 for the 20- and 10-mg/kg doses (Fig. 2B–E).

In the watermaze, CCI mice receiving BQCA demonstrated significantly decreased latency during week 3 (DOSE×DAYS, week 3, $F_{3,37}=6.8$; $p<0.001$), with a nonsignificant trend during weeks 1 and 2. A similar pattern was observed for the pathlength variable (DOSE×DAYS, week 3, $F_{3,37}=3.6$; $p<0.02$). Post-hoc

testing during week 3 showed the CCI-Veh compared to CCI-20 dose to have significantly lower latencies during days 2–4 ($p < 0.05$), as well as shorter pathlengths during days 3–4 ($p < 0.05$), with a nonsignificant trend at other time points and at lower BQCA doses. During the probe trial (Fig. 3), percentage of time spent swimming in the target quadrant showed no significant difference between the Sham-Veh, CCI-5, CCI-10, and CCI-20 groups.

Effect of lesion on cerebral glucose metabolic response during wheel walking

Lesioned compared to sham-lesioned animals showed a significant decrease in rCGU broadly across the lesioned hemisphere (Fig. 5; Table 1). In the motor circuit, significant decreases in rCGU were noted in the ipsilesional striatum across anterior to posterior sites, with greatest decreases noted dorsally, but also with involvement ventrally, and relative sparing of the central zone. Significantly decreased rCGU was noted also in the ipsilesional anterior motor cortex (primary, secondary), external globus pallidus, motor thalamus (mediodorsal, ventral anterior, ventrolateral, ventromedial), subthalamic nucleus, and zona incerta. Lesioned compared to sham lesioned animals showed a significant increase in rCGU primarily in the contralateral, nonlesioned hemisphere. In the contralesional motor circuit, lesioned compared to sham-lesioned mice showed a significantly increased rCGU in anterior primary motor cortex, striatum (anterior to posterior), external globus pallidus, zona incerta, red nucleus, as well as in the centromedial thalamus. A significantly greater rCGU was also noted bilaterally in the cerebellum (lateral cerebellum, deep cerebellar nuclei, and vermis). Within the somatosensory system, significant decreases in rCGU were noted in ipsilesional somatosensory cortex (primary, secondary) and sensory thalamus (e.g., posterior, ventroposterior lateral, and ventroposterior medial nuclei), with significantly increased rCGU noted contralesionally in these regions. Lesions differentially changed rCGU in the hippocampal formation, with significant decreases noted bilaterally in the anterior dentate gyrus, and ipsilesional subiculum, and significant increases noted broadly in contralesional CA1 (anterior, posterior), dentate gyrus (posterior), and the subiculum. Outside these systems, significantly decreased cortical rCGU was also noted in the ipsilesional midline cortex (cingulate, prelimbic, and retrosplenial), in orbital (lateral, ventral), anterior auditory, and secondary visual cortices, with significant increases noted in bilateral infralimbic and ipsilesional insular cortex. Subcortical changes included a significantly decreased rCGU in the bilateral inferior colliculus, ipsilesional thalamus (lateral dorsal, lateral posterior, anterior dorsal, anterior medial, and anterior ventral, reticular), dorsolateral geniculate, anterior pretectal area, and amygdala (central, lateral nuclei). Significantly increased rCGU was broadly noted contralesionally in the amygdala (basal, central, lateral, medial, and cortical nuclei), hypothalamus (anterior, lateral, medial/lateral preoptic, posterior, and ventromedial nuclei), thalamus (lateral posterior, reticular nuclei), as well as bilaterally in the nucleus accumbens, reticular formation, pons, and vestibular nuclei.

Effect of benzylquinolone carboxylic acid in cortical contusion injury mice on cerebral glucose metabolic response during motor wheel walking

For mice exposed to CCI, BQCA compared to vehicle treatment resulted in modest, though significantly increased, rCGU in motor regions, including bilateral secondary motor cortex (ipsilesional > contralesional), posterior contralesional striatum, and the motor thalamus (bilateral ventrolateral/ventromedial nuclei, contralesional ventral anterior, and mediodorsal nuclei), with significant decreases in the contralesional substantia nigra, zona incerta, red nucleus, and the bilateral cerebellum (lateral lobe, deep cerebellar nuclei, and vermis). BQCA differentially changed rCGU in the hippocampal formation with broad and significant increases in ipsilesional CA1-3 (posterior), contralesional dentate gyrus (anterior), and significant decreases in contralesional CA1 (anterior, posterior). Significantly increased rCGU was noted in bilateral midline (cingulate, prelimbic) and orbital (lateral, ventral) cortices, in contralesional retrosplenial, primary somatosensory, and visual cortices, as well as in the contralesional, sensory thalamus (ventroposterior medial, ventroposterior lateral nuclei). Significant decreases in rCGU were noted in the amygdala (bilateral basolateral, central, cortical nuclei, and the ipsilesional lateral nucleus), the bilateral nucleus accumbens, ventromedial hypothalamus, and vestibular nuclei.

rCGU in the ipsilesional hippocampal CA1 field showed a significant negative correlation with latency to find the platform on the final day of week 3 and a positive correlation with rCGU contralesionally (Fig. 6). Similar significant results were obtained for the correlation of pathlength with rCGU (data not shown).

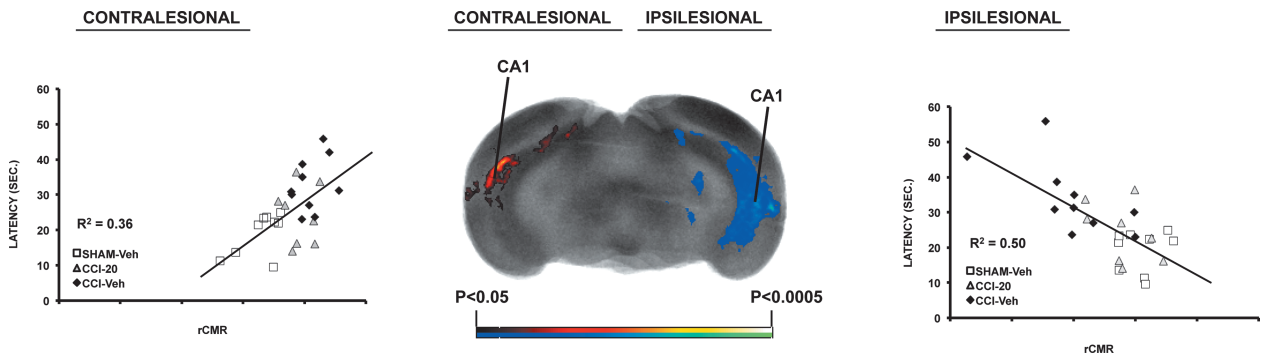

FIG. 6. Correlation of spatial learning and rCGU. Significant correlations between the latency to find the submerged platform in the water maze on day 4 of week 3 and rCGU across the combined Sham-Veh, CCI-Veh, and CCI-20 groups ($n = 8$–10 per group). The center image is a representative coronal section at the level of the posterior CA1 region that shows correlation of rCGU at the voxel level ($p < 0.05$) for clusters of >100 contiguous voxels. Right and left graphs, respectively, depict ipsi- and contralesional correlations of latency with relative cerebral metabolism of a region of interest within the posterior CA1 region. CCI, cortex contusion injury; rCGU, regional brain glucose uptake; Veh, vehicle.

Discussion

Effects of cortical contusion injury and benzylquinolone carboxylic acid on behavior

Unilateral CCI resulted in a significant, persistent, asymmetric postural reflex on tail suspension. Motor testing revealed significant deficits on the accelerating rotarod, increased footslips on grid walking and decreased grip strength ($p < 0.05$) throughout the 3-week follow-up period. Effects of BQCA on motor outcomes were minimal. There was a trend toward the highest dose of BQCA attenuating the locomotor hyperactivity in the open field noted in CCI animals. In nonlesioned animals, BQCA at 20 mg/kg showed no significant effect on general motor activity, body weight, or acute motor, secretory, or respiratory symptoms.

Compared to SHAM-Veh controls, CCI-Veh mice demonstrated significantly delayed spatial learning at 3 weeks post-CCI during exposure to a reverse learning task in which the platform position was moved ($p < 0.05$). In our CCI mice, BQCA resulted in improved spatial learning and recall over time, with significant changes noted during the final days of the third week for the highest dose. The highest dose of BQCA (but not the low or medium doses) also resulted in a significant decrease in lesion size, a trend previously reported by us in a rat CCI model after chronic physostigmine infusion.[10]

Effects of cortical contusion injury and benzylquinolone carboxylic acid on cerebral glucose uptake

Most studies that have examined rCGU in the awake animal after TBI have focused on changes occurring at <24 h post-injury. Our study examined cerebral glucose uptake in the awake mouse during a motor challenge 1 month after CCI injury. CCI overlying the right motorsensory cortex resulted in broad decreases in rCGU in the basal ganglia/thalamocortical circuit ipsilesionally, including loss of activation of the motor cortex, striatum, external globus pallidus, subthalamic nucleus, and motor thalamus. These results are in agreement with human and animal work that has documented chronic decreases in rCGU after TBI.[45–47] In the contralesional hemisphere, CCI elicited relative increases in rCGU, with significant functional recruitment of stations within the classical basal ganglia circuit, including anterior primary motor cortex, striatum (anterior → posterior), external globus pallidus, motor thalamus, and in the red nucleus, as well as the bilateral cerebellum. Findings complement those previously reported by us using cerebral perfusion mapping for changes in functional activation of the motor system in the rat after CCI.[10] Additional decreases in rCGU were noted in ipsilesional somatosensory regions, including the primary and secondary somatosensory cortices and sensory thalamus, and with significant relative increases noted contralesionally. In the hippocampus, CCI resulted in significant decreases in rCGU of the ipsilesional CA1, dentate gyrus, and dorsal subiculum, with significant increases noted contralesionally in CA1 (anterior, posterior), dentate gyrus (posterior), and the subiculum. Our study supports earlier findings delineated by perfusion and by metabolic mapping that focal TBI can result in persistent global functional changes of neuronal networks that extend beyond the obvious lesion site.[8,10,48]

Transhemispheric reorganization after localized injury is well known,[49–51] a phenomena within the field of processes known as "diaschisis."[52] In our study, the regional distribution of the transhemispheric rCGU enhancement was not limited to the sensorimotor regions homologous to those that show injury and permanent damage in this model, but it extended to subcortical regions such as the thalamus, hippocampus, as well as distant regions, including visual and auditory cortex, as well as the cerebellum, suggesting extensive functional adaptation. Earlier work by Weil and colleagues[46] in a mouse model of single closed TBI also demonstrated contralesional increases in rCGU in motor cortex and the thalamus, but without persistence beyond day 6 post-injury. Differences in the TBI model and/or mouse strain likely contribute to these divergent findings.

Chronic administration of BQCA (20 mg/kg) resulted in modest changes in rCGU, which attenuated the rCGU changes after CCI noted in isolated motor, sensory, and hippocampal regions. In the motor system, BQCA significantly diminished the contralesional increases in rCGU of individual motor regions (red nucleus, zona incerta, and substantia nigra), as well as broadly across the cerebellum. Significant ipsilesional increases by BQCA of the CCI-associated decreases in rCGU was noted only in secondary motor cortex and the ventrolateral and ventromedial motor nuclei of the thalamus. Despite the changes in rCGU elicited in the motor circuit by BQCA, there were, as noted above, few, if any, improvements in gross motor function associated with drug treatment. A significant improvement in footslip performance was noted in mice receiving BQCA 1 week after CCI, but thereafter performance remained at the level of a nonsignificant trend, with a similar finding noted for the open field test. In the hippocampus, BQCA attenuated some of the changes noted in response to CCI, with significant decreases in rCGU in contralesional CA1 (anterior, posterior), and significant increases in the contralesional dentate gyrus (anterior) and ipsilesional CA2-3 (posterior). As noted above, BQCA's effects were more pronounced in the spatial learning outcomes than on the motor outcomes, a finding which we have previously noted in CCI rats treated with physostigmine.[53,54] Our findings showed a significant correlation between measures of spatial learning (latency, pathlength) and rCGU in posterior CA1, with a negative correlation ipsilesionally and a positive correlation contralesionally. Thus, longer latencies were associated with a lower ipsilesional rCGU and with a higher contralesional rCGU. This suggests that latency inversely correlates with metabolic deficits on the side of the lesion, and directly correlates with a state of relative increased glucose uptake contralesionally, possibly as a compensatory response. Additional work would need to be done to confirm this in a paradigm in which imaging is performed during spatial learning. The fact that the BQCA effect was greatest in the final week of testing suggests that the injured brain remains receptive at this late time point to pharmacological intervention.

BQCA significantly increased rCGU in the bilateral medial prefrontal cortex (cingulate, prelimbic), a finding consistent with a previous report of BQCA's *in vivo* excitatory effects on medial prefrontal regions.[24] Shirey and colleagues have proposed that excitation of M1 receptors in medial prefrontal cortex by BQCA may be related to its effects on cognitive function, specifically discrimination reversal learning,[24] a factor which may also have contributed to our finding that BQCA improves reversal learning in the water maze.

Conclusion

BQCA in CCI mice elicited improved hippocampal-dependent learning in a spatial navigation task that included reversal of the target position. Improvements were noted in the absence of significant cholinergic side effects. No significant drug effect was noted on motor outcomes. These results suggest that BQCA is a candidate compound to improve learning and memory function

after brain trauma, and may not suffer the associated central nervous system side effects typically associated with even modest doses of other cholinergic enhancers. Of note, increasing BQCA doses did not elicit a worsening of outcomes, as has previously noted for motor outcomes with physostigmine.[53]

Some limitations of this study and its interpretation should be addressed. Effects on improved hippocampal-dependent learning were modest. It is possible that greater beneficial effects on cognitive function may have been observed at higher doses of BQCA or more prolonged treatment, though the 20–30 mg/kg is typically the maximum dose reported in the pre-clinical literature. Future studies should examine the application of BQCA in milder forms of TBI (i.e. closed concussive TBI), given that it is possible that greater responsivity might be achieved here. A more extensive evaluation of side-effect profiles should be conducted also in lesioned animals.

Acknowledgments

We commemorate the life and scientific work Oscar U. Scremin, MD, PhD, a friend and mentor, who passed away during completion of this study. The current research was supported by a grant from the National Institutes of Neurologic Disorders and Stroke (NINDS) 5R21NS096554.

Author Disclosure Statement

No competing financial interests exist.

References

1. Gold, P.E. (2003). Acetylcholine modulation of neural systems involved in learning and memory. Neurobiol. Learn. Mem. 80, 194–210.
2. Ostberg, A., Virta, J., Rinne, J.O., Oikonen, V., Luoto, P., Nagren, K., Arponen, E., and Tenovuo, O. (2011). Cholinergic dysfunction after traumatic brain injury: preliminary findings from a PET study. Neurology 76, 1046–1050.
3. Scremin, O.U., Li, M.G., Roch, M., Booth, R., and Jenden, D.J. (2006). Acetylcholine and choline dynamics provide early and late markers of traumatic brain injury. Brain Res. 1124, 155–166.
4. Donat, C.K., Schuhmann, M.U., Voigt, C., Nieber, K., Deuther-Conrad, W., and Brust, P. (2008). Time-dependent alterations of cholinergic markers after experimental traumatic brain injury. Brain Res. 1246, 167–177.
5. Donat, C.K., Walter, B., Deuther-Conrad, W., Wenzel, B., Nieber, K., Bauer, R., and Brust, P. (2010). Alterations of cholinergic receptors and the vesicular acetylcholine transporter after lateral fluid percussion injury in newborn piglets. Neuropathol. Appl. Neurobiol. 36, 225–236.
6. Hoffmeister, P.G., Donat, C.K., Schuhmann, M.U., Voigt, C., Walter, B., Nieber, K., Meixensberger, J., Bauer, R., and Brust, P. (2011). Traumatic brain injury elicits similar alterations in alpha7 nicotinic receptor density in two different experimental models. Neuromolecular Med. 13, 44–53.
7. Valiyaveettil, M., Alamneh, Y.A., Miller, S.A., Hammamieh, R., Arun, P., Wang, Y., Wei, Y., Oguntayo, S., Long, J.B., and Nambiar, M.P. (2013). Modulation of cholinergic pathways and inflammatory mediators in blast-induced traumatic brain injury. Chem. Biol. interact. 203, 371–375.
8. Scremin, O.U., Li, M.G., and Scremin, A.M. (2007). Cortical contusion induces trans-hemispheric reorganization of blood flow maps. Brain Res. 1141, 235–241.
9. Scremin, O.U., Li, M.G., and Jenden, D.J. (1997). Cholinergic modulation of cerebral cortical blood flow changes induced by trauma. J. Neurotrauma 14, 573–586.
10. Holschneider, D.P., Guo, Y., Wang, Z., Roch, M., and Scremin, O.U. (2013). Remote brain network changes after unilateral cortical impact injury and their modulation by acetylcholinesterase inhibition. J. Neurotrauma 30, 907–919.
11. Tenovuo, O. (2005). Central acetylcholinesterase inhibitors in the treatment of chronic traumatic brain injury-clinical experience in 111 patients. Prog. Neuropsychopharmacol. Biol. Psychiatry 29, 61–67.
12. Griffin, S.L., van Reekum, R. and Masanic, C. (2003). A review of cholinergic agents in the treatment of neurobehavioral deficits following traumatic brain injury. J. Neuropsychiatry Clin. Neurosci. 15, 17–26.
13. Khateb, A., Ammann, J., Annoni, J.M., and Diserens, K. (2005). Cognition-enhancing effects of donepezil in traumatic brain injury. Eur. Neurol. 54, 39–45.
14. Kim, Y.W., Kim, D.Y., Shin, J.C., Park, C.I., and Lee, J.D. (2009). The changes of cortical metabolism associated with the clinical response to donepezil therapy in traumatic brain injury. Clin. Neuropharmacol. 32, 63–68.
15. Zhang, L., Plotkin, R.C., Wang, G., Sandel, M.E., and Lee, S. (2004). Cholinergic augmentation with donepezil enhances recovery in short-term memory and sustained attention after traumatic brain injury. Arch. Phys. Med. Rehabil. 85, 1050–1055.
16. Inglis, F. (2002). The tolerability and safety of cholinesterase inhibitors in the treatment of dementia. International journal of clinical practice. Suppl. 127, 45–63.
17. Leroi, I., Brandt, J., Reich, S.G., Lyketsos, C.G., Grill, S., Thompson, R., and Marsh, L. (2004). Randomized placebo-controlled trial of donepezil in cognitive impairment in Parkinson's disease. Int. J. Geriatr. Psychiatry 19, 1–8.
18. Thompson, S., Lanctot, K.L., and Herrmann, N. (2004). The benefits and risks associated with cholinesterase inhibitor therapy in Alzheimer's disease. Exp. Opin. Drug Saf. 3, 425–440.
19. Shin, S.S., and Dixon, C.E. (2015). Alterations in cholinergic pathways and therapeutic strategies targeting cholinergic system after traumatic brain injury. J. Neurotrauma 32, 1429–1440.
20. Abdul-Ridha, A., Lopez, L., Keov, P., Thal, D.M., Mistry, S.N., Sexton, P.M., Lane, J.R., Canals, M., and Christopoulos, A. (2014). Molecular determinants of allosteric modulation at the M1 muscarinic acetylcholine receptor. J. Biol. Chem. 289, 6067–6079.
21. Foster, D.J., Choi, D.L., Conn, P.J., and Rook, J.M. (2014). Activation of M and M muscarinic receptors as potential treatments for Alzheimer's disease and schizophrenia. Neuropsychiatr. Dis. Treat. 10, 183–191.
22. Uteshev, V.V. (2014). The therapeutic promise of positive allosteric modulation of nicotinic receptors. Eur. J. Pharmacol. 727, 181–185.
23. Chambon, C., Jatzke, C., Wegener, N., Gravius, A., and Danysz, W. (2012). Using cholinergic M1 receptor positive allosteric modulators to improve memory via enhancement of brain cholinergic communication. Eur. J. Pharmacol. 697, 73–80.
24. Shirey, J.K., Brady, A.E., Jones, P.J., Davis, A.A., Bridges, T.M., Kennedy, J.P., Jadhav, S.B., Menon, U.N., Xiang, Z., Watson, M.L., Christian, E.P., Doherty, J.J., Quirk, M.C., Snyder, D.H., Lah, J.J., Levey, A.I., Nicolle, M.M., Lindsley, C.W., and Conn, P.J. (2009). A selective allosteric potentiator of the M1 muscarinic acetylcholine receptor increases activity of medial prefrontal cortical neurons and restores impairments in reversal learning. J. Neurosci. 29, 14271–14286.
25. Ma, L., Seager, M.A., Wittmann, M., Jacobson, M., Bickel, D., Burno, M., Jones, K., Graufelds, V.K., Xu, G., Pearson, M., McCampbell, A., Gaspar, R., Shughrue, P., Danziger, A., Regan, C., Flick, R., Pascarella, D., Garson, S., Doran, S., Kreatsoulas, C., Veng, L., Lindsley, C.W., Shipe, W., Kuduk, S., Sur, C., Kinney, G., Seabrook, G.R., and Ray, W.J. (2009). Selective activation of the M1 muscarinic acetylcholine receptor achieved by allosteric potentiation. Proc. Natl. Acad. Sci. U. S. A. 106, 15950–15955.
26. Uslaner, J.M., Eddins, D., Puri, V., Cannon, C.E., Sutcliffe, J., Chew, C.S., Pearson, M., Vivian, J.A., Chang, R.K., Ray, W.J., Kuduk, S.D., and Wittmann, M. (2013). The muscarinic M1 receptor positive allosteric modulator PQCA improves cognitive measures in rat, cynomolgus macaque, and rhesus macaque. Psychopharmacology (Berl) 225, 21–30.
27. Chambon, C., Wegener, N., Gravius, A., and Danysz, W. (2011). A new automated method to assess the rat recognition memory: validation of the method. Behav. Brain Res. 222, 151–157.
28. Jovic, R.C. (1974). Correlation between signs of toxicity and some biochemical changes in rats poisoned by soman. Eur. J. Pharmacol. 25, 159–164.
29. Senda, D.M., Franzin, S., Mori, M.A., de Oliveira, R.M., and Milani, H. (2011). Acute, post-ischemic sensorimotor deficits correlate positively with infarct size but fail to predict its occurrence and magnitude

after middle cerebral artery occlusion in rats. Behav. Brain Res. 216, 29–35.
30. Carter, R.J., Morton, J., and Dunnett, S.B. (2001). Motor coordination and balance in rodents. Curr. Protoc. Neurosci. Chapter 8, Unit 8 12. doi: 10.1002/0471142301.ns0812s15.
31. Rozas, G., Lopez-Martin, E., Guerra, M.J., and Labandeira-Garcia, J.L. (1998). The overall rod performance test in the MPTP-treated-mouse model of Parkinsonism. J. Neurosci. Methods 83, 165–175.
32. Wang, Z., Stefanko, D.P., Guo, Y., Toy, W.A., Petzinger, G.M., Jakowec, M.W., and Holschneider, D.P. (2016). Evidence of functional brain reorganization on the basis of blood flow changes in the CAG140 knock-in mouse model of Huntington's disease. Neuroreport 27, 632–639.
33. Morris, R. (1984). Developments of a water-maze procedure for studying spatial learning in the rat. J. Neurosci. Methods 11, 47–60.
34. Holschneider, D.P., Scremin, O.U., Chen, K., and Shih, J.C. (1999). Lack of protection of monoamine oxidase B-deficient mice from age-related spatial learning deficits in the Morris water maze. Life Sci. 65, 1757–1763.
35. Sokoloff, L., Reivich, M., Kennedy, C., Des Rosiers, M.H., Patlak, C.S., Pettigrew, K.D., Sakurada, O., and Shinohara, M. (1977). The [14C]deoxyglucose method for the measurement of local cerebral glucose utilization: theory, procedure, and normal values in the conscious and anesthetized albino rat. J. Neurochem. 28, 897–916.
36. Melzer, P., Van der Loos, H., Dorfl, J., Welker, E., Robert, P., Emery, D., and Berrini, J.C. (1985). A magnetic device to stimulate selected whiskers of freely moving or restrained small rodents: its application in a deoxyglucose study. Brain Res. 348, 229–240.
37. Jordan, G.R., McCulloch, J., Shahid, M., Hill, D.R., Henry, B., and Horsburgh, K. (2005). Regionally selective and dose-dependent effects of the ampakines Org 26576 and Org 24448 on local cerebral glucose utilisation in the mouse as assessed by 14C-2-deoxyglucose autoradiography. Neuropharmacology 49, 254–264.
38. Vyazovskiy, V.V., Cirelli, C., Tononi, G., and Tobler, I. (2008). Cortical metabolic rates as measured by 2-deoxyglucose-uptake are increased after waking and decreased after sleep in mice. Brain Res. Bull. 75, 591–597.
39. Thevenaz, P., Ruttimann, U.E., and Unser, M. (1998). A pyramid approach to subpixel registration based on intensity. IEEE Trans. Image Process 7, 27–41.
40. Nguyen, P.T., Holschneider, D.P., Maarek, J.M., Yang, J., and Mandelkern, M.A. (2004). Statistical parametric mapping applied to an autoradiographic study of cerebral activation during treadmill walking in rats. Neuroimage 23, 252–259.
41. Brett, M., Leff, A.P., Rorden, C., and Ashburner, J. (2001). Spatial normalization of brain images with focal lesions using cost function masking. Neuroimage 14, 486–500.
42. Ripolles, P., Marco-Pallares, J., de Diego-Balaguer, R., Miro, J., Falip, M., Juncadella, M., Rubio, F., and Rodriguez-Fornells, A. (2012). Analysis of automated methods for spatial normalization of lesioned brains. Neuroimage 60, 1296–1306.
43. Friston, K., and the Methodology group at the Wellcome Dept.of Cognitive Neurology. (1999). Statistical Parametric Mapping (SPM99). www.fil.ion.ucl.ac.uk/spm/ (last accessed March 14, 2019).
44. Franklin, K.B.J., and Paxinos, G. (2007). *The Mouse Brain in Stereotaxic Coordinates*, 3rd ed. Academic: New York.
45. Nakayama, N., Okumura, A., Shinoda, J., Nakashima, T., and Iwama, T. (2006). Relationship between regional cerebral metabolism and consciousness disturbance in traumatic diffuse brain injury without large focal lesions: an FDG-PET study with statistical parametric mapping analysis. J. Neurol. Neurosurg. Psychiatry 77, 856–862.
46. Weil, Z.M., Gaier, K.R., and Karelina, K. (2014). Injury timing alters metabolic, inflammatory and functional outcomes following repeated mild traumatic brain injury. Neurobiol. Dis. 70, 108–116.
47. Yoshino, A., Hovda, D.A., Kawamata, T., Katayama, Y., and Becker, D.P. (1991). Dynamic changes in local cerebral glucose utilization following cerebral conclusion in rats: evidence of a hyper- and subsequent hypometabolic state. Brain Res. 561, 106–119.
48. Dietrich, W.D., Alonso, O., Busto, R., and Ginsberg, M.D. (1994). Widespread metabolic depression and reduced somatosensory circuit activation following traumatic brain injury in rats. J. Neurotrauma 11, 629–640.
49. Clarey, J.C., Tweedale, R., and Calford, M.B. (1996). Interhemispheric modulation of somatosensory receptive fields: evidence for plasticity in primary somatosensory cortex. Cereb. Cortex 6, 196–206.
50. Zarei, M., Raevsky, V.V., Dawe, G.S., and Stephenson, J.D. (2001). Changes in sensitivity of cholinoceptors and adrenoceptors during transhemispheric cortical reorganisation in rat SmI. Brain Res. 888, 267–274.
51. Zarei, M., and Stephenson, J.D. (2000). Transhemispheric cortical reorganization in rat SmI and involvement of central noradrenergic system. Brain Res. 870, 142–149.
52. Meyer, J.S., Hata, T., and Imai, A. (1987). Clinical and experimental studies of diaschisis, in: *Cerebral Blood Flow: Physiologic and Clinical Aspects*. J.H. Wood (ed). McGraw-Hill: New York, pps. 481–502.
53. Holschneider, D.P., Guo, Y., Roch, M., Norman, K.M., and Scremin, O.U. (2011). Acetylcholinesterase inhibition and locomotor function after motor-sensory cortex impact injury. J. Neurotrauma 28, 1909–1919.
54. Scremin, O.U., Norman, K.M., Roch, M., Holschneider, D.P., and Scremin, A.M. (2012). Acetylcholinesterase inhibition interacts with training to reverse spatial learning deficits of cortical impact injury. J. Neurotrauma 29, 2457–2464.
55. Franklin, K.B.J., and Paxinos, G. (2007). *The Mouse Brain in Stereotactic Coordinates*, 3rd ed. Academic: San Diego, CA.

Address correspondence to:
Daniel P. Holschneider, MD
Department of Psychiatry and the Behavioral Sciences
University of Southern California
1975 Zonal Avenue
KAM 400, MC9037
Los Angeles, CA 90089-9037

E-mail: holschne@usc.edu